Nano Research 2015, 8(8): 2481–2491
DOI 10.1007/s12274-015-0756-4
Research Article

ISSN 1998-0124
CN 11-5974/O4

Energy harvesting model of moving water inside a tubular system and its application of a stick-type compact triboelectric nanogenerator

Dongwhi Choi[1,§], Sangmin Lee[2,§], Sang Min Park[1], Handong Cho[1], Woonbong Hwang[1], and Dong Sung Kim[1] (✉)

[1] *Department of Mechanical Engineering, Pohang University of Science and Technology (POSTECH), 77 Cheongam-ro, Pohang, Gyeongbuk, 790-784, Republic of Korea*
[2] *School of Mechanical Engineering, Chung-Ang University, 84 Heukseok-ro, Dongjak-gu, Seoul, 156-756, Republic of Korea*
[§] *These authors contributed equally to this work.*

Received: 21 January 2015
Revised: 20 February 2015
Accepted: 26 February 2015

KEYWORDS

contact electrification,
triboelectric nanogenerator,
anodized aluminum xide,
superhydrophobic tubular system,
compact design

ABSTRACT

As the first invention to efficiently harvest electricity from ambient mechanical energy by using contact electrification, the triboelectric nanogenerator has elicited worldwide attention because of its cost-effectiveness and sustainability. This study exploits a superhydrophobic nanostructured aluminum tube to estimate electrical output for solid–water contact electrification inside a tubular system. The linearly proportional relationship of short-circuit current and open-circuit voltage to the detaching speed of water was determined by using a theoretical energy harvesting model and experimentation. A pioneering stick-type solid–water interacting triboelectric nanogenerator, called a SWING stick, was developed to harvest mechanical energy through solid–water contact electrification generated when the device is shaken by hand. The electrical output generated by various kinds of water from the environment was also measured to demonstrate the concept of the SWING stick as a compact triboelectric nanogenerator. Several SWING sticks were connected to show the feasibility of the device as a portable and compact source of direct power. The developed energy harvesting model and the SWING stick can provide a guideline for the design parameters to attain a desired electrical output; therefore, this study can significantly increase the applicability of a water-driven triboelectric nanogenerator.

1 Introduction

The rapid increase in human population has led to excessive consumption of fossil fuels. With the limited supply of fossil fuels, sustainable and renewable energy has been widely emphasized and studied recently [1–3]. As a result, the triboelectric nanogenerator (TENG), the first invention that utilizes contact electrification

Address correspondence to Dong Sung Kim, smkds@postech.ac.kr

to efficiently harvest mechanical energy into electrical energy, has elicited worldwide attention [4–7].

Contact electrification, known as triboelectricity, is a process of spontaneous charge generation on two surfaces separated after having been in contact. However, despite its thousands of years of history, the exact mechanism has remained unclear [8–11]. The TENG can generate electrical output with high efficiency using cyclic contact and separation of two materials with different triboelectric polarities. The output level of the TENG is significantly increased with the use of a solid-phase polymer with high triboelectric polarity and nanostructured materials [12–14]. Until 2013, the TENG normally utilized two solid-phase polymers as contact materials because of their high triboelectric polarity and concomitant high electrical output level. Therefore, a conventional TENG system works in a relatively dry environment to provide stable electrical output, because the presence of water would significantly suppress the solid–solid contact electrification phenomenon [15, 16].

Recently, our group has firstly reported that conventional pipetting spontaneously generates a considerable amount of electric charge (on the order of 0.1 nC), depending on the constituents of the droplet, atmospheric humidity, and coating material of the inner surface of the pipette tip [17, 18]. When the aqueous solution comes into contact with the inner surface of the pipette tip, spontaneous electrification occurs due to the ionization of the surface chemical groups on the polymeric pipette tip. In other words, triboelectricity does exist when water contacts the polymeric surface. Using this idea, a water-driven TENG utilizing solid–water contact electrification was first suggested by Wang's group in 2013 [19]. The electrical output of a water-driven TENG, which is sufficiently large to light up commercial light-emitting diodes (LED), can be achieved by a periodic contact and separation process between water and patterned poly-dimethylsiloxane (PDMS) via a motorized system. Given the nature of water, a water-driven TENG has several advantages, such as independence with humidity and robustness, compared to conventional TENGs designed for contact among solid materials. The water-driven TENG has been developed to harvest several forms of water energy, such as water wave, vibration, flowing water, and water drop energy [6, 13, 20–23]. However, because of the unconstrained movement of the water, all previous studies on the water-driven TENG are unsuitable for a compact design. Because a compact design for the TENG is essential for achieving evaporation-free and contamination-free conditions, it would enable long-lasting operation with a fixed amount of water. In addition, with respect to the previously studied unconstrained type of water-driven TENG, it was difficult to vary the detaching speed of the water to explore its effect on electrical output. Even the only report on the effect of the contact frequency on the output voltage failed to determine the relationship because of the generated fluctuating wave on the surface during the operation [19]. Therefore, compact design is an important factor for the water-driven TENG, because water has high fluidity compared to solid materials.

In this work, the anodized aluminum oxide nanostructures on a curved aluminum surface (tube) are utilized to fabricate the superhydrophobic nanostructured aluminum tube. The effect of the detaching speed of the water on the electrical output will then be explored. The linearly proportional relationship of short-circuit current and open-circuit voltage to the detaching speed of water will be determined using a charge-based energy harvesting model and experimentation. The developed charge-based energy harvesting model can also provide a guideline for the design parameters required to attain a desired electrical output using solid–water contact electrification. Utilizing the tubular system, the pioneering stick-type solid–water interacting triboelectric nanogenerator, or "SWING stick," is suggested and demonstrated to harvest mechanical energy generated when the device is shaken by hand. The compact design of the SWING stick can achieve the evaporation-free and contamination-free condition necessary for long-lasting and stable operation with a fixed amount of water. The output generated from 2 mL water can achieve a peak voltage of 30 V and a peak current of 2 μA via hand-shaking. By including several types of water (deionized water, rain, seawater, and electrolyte solution), this study demonstrates the concept of the SWING stick, which can be used to harvest hand-shaking mechanical energy with various kinds of water from the environment. The parallel connection of SWING sticks, called a “SWING pack,” enables easy amplification of electrical output sufficient to power 15 conventional LEDs. Given that the fundamental mechanism of solid–water contact electrification can be easily explored with the help of the SWING stick’s compact design, resulting in high controllability, the applicability of nanogenerators using solid–water contact electrification can be significantly increased.

2 Experimental

2.1 Materials

The deionized water, oxalic acid, and n-hexane were supplied from SAMCHUN Chemical, Korea. The heptadecafluoro-1,1,2,2-tetrahydrodecyl trichlorosilane (HDFS) was purchased from Gelest, Inc., USA. The 6 wt% solution of Teflon AF 1600 (Du Pont, Wilmington, DE) was diluted to 1 wt% with FC-40 (Du Pont, Wilmington, DE).

2.2 Fabrication of the superhydrophobic nanostructures on a three-dimensionally curved aluminum surface

The conventional aluminum tube was ultrasonically cleaned in ethanol and deionized water. Hierarchical micro/nanostructures on the tube were then fabricated through a single-step anodization process. Anodization was conducted using 0.3 M oxalic acid at 70 V for 6 h according to a previously published method [24]. In order to provide superhydrophobic properties to the as-prepared specimen, the surface was chemically modified using a self-assembled monolayer (SAM) of HDFS. The specimen was dipped in a 0.1% (V/V) n-hexane solution of HDFS at room temperature for 10 min, followed by drying at 110 °C for 10 min. The diluted Teflon was added to the surface to form an overcoated Teflon layer.

2.3 Effective surface charge density measurement

Because the amount of the developed charge on the superhydrophobic nanostructures was the same as that of the solution, we measured the charge of the solution dispensed by the fabricated tube rather than the charge on the inner surface of the superhydrophobic nanostructured aluminum tube. The Faraday cup method was used to measure the charge developed by solid-water contact electrification. The charge was directly measured by using a Faraday cup connected to an electrometer (Keithley Model 6517A). The charged solution was dispensed from the syringe, and the effective surface charge density was calculated. Detailed information can be found in the ESM.

3 Results and Discussion

3.1 Superhydrophobic nanostructured aluminum tube for energy harvesting

A superhydrophobic nanostructured aluminum tube was fabricated to harvest mechanical energy using solid–water contact electrification as shown in Fig. 1(a). The contact angle of the water droplet sitting on the as-treated surface was measured with SmartDrop (Femtofab, Korea) to determine the superhydrophobicity of the surface and the measured contact angle, which was approximately 170°. The detailed result can be found in the ESM. The nanostructured aluminum tube was manufactured based on an electrochemical oxidation process (also called anodization) conducted on a conventionally available aluminum tube (inner diameter of 6 mm), resulting in an anodized aluminum oxide (AAO) layer. The AAO layer was coated with Teflon solution. The scanning electron microscopic (SEM) image in Fig. 1(a) shows that the outermost part of the inner surface of the tube is composed of the Teflon-coated nanostructures, which acts as a superhydrophobic nanostructured dielectric layer. The nanostructured surface modification enhances the output of the SWING, and the excellent mechanical properties of aluminum oxide ensure robustness [19–21]. Details of the fabrication process are stated in the experimental section. To the best of our knowledge, this was the first utilization of AAO nanostructures fabricated on a three-dimensionally curved aluminum surface as a water-driven TENG. The half of the outer surface of the tube was not anodized for electrical connection. The reservoir was filled with water, and the aluminum tube was electrically connected to the water inside the reservoir. The syringe plunger was connected and sealed to the end of the tube to effect the movement of water through the tube (Fig. 1(b)). Operation of the fabricated tube relied on a repetitive aspirating-dispensing process with moving water inside the tube, which induced the unique coupling of contact electrification and electrostatic induction. In general, it has been found that contact between water and a material with negative triboelectric polarity (e.g., Teflon) induces negative charges at the contact interface of the material and positive charges at the interface of the water. However, the exact fundamental mechanism of charge development remains unclear [17, 25, 26]. In the case of a hydrophobic material, the positive and negative charges at the interface can be easily separated with the detachment of water from the material. Therefore, the hydrophobicity of the material can be considered to be a key parameter for charge separation, resulting in electron flow. Given that the separated negative charges at the contact interface of the material are not dissipated for an extended period, the electrons have the tendency to move far from the interface because of the electrical repulsion force. This natural flow of electrons generates current and electrical energy. In our experimental case, the electrons flowed through the electric wire from the reservoir to the aluminum tube and vice versa. For quantitative analysis, the programmable rotary motor and the linear guide were connected to the syringe plunger to achieve controlled plunger velocity.

Figure 1(b) < i > shows that the water aspirating from the reservoir through the tube can be acquired by pulling the plunger. In addition, concomitant contact between the outermost part of the inside of the aluminum tube (namely, the superhydrophobic nanostructured surface and aspirated water) induced charges at the interface. Pushing the plunger dispensed water inside the tube. The Teflon-coated nanostructured surface with superhydrophobic properties allowed easy charge separation, thereby enhancing electrical output [20, 21]. As the water moved toward the reservoir, the developed negative charges at the surface remained, and the electrons inside the aluminum tube near the contact interface moved to the reservoir through the connected wire. The resultant positive charges inside the aluminum tube can screen the remaining negative charges at the superhydrophobic surface, satisfying the electroneutrality inside the system. This movement of electrons through the wire generates current, as shown in Fig. 1(b) < ii >. Figure 1(b) < iii > corresponds to the state at which all developed negative charges were screened by the positive charges inside the aluminum tube and no more current could be generated. By pulling the plunger again, current with opposite direction could be produced. As the water entered the tube, the negative charges at the surface preferred to be screened by the positive charges inside the water because of the short distance

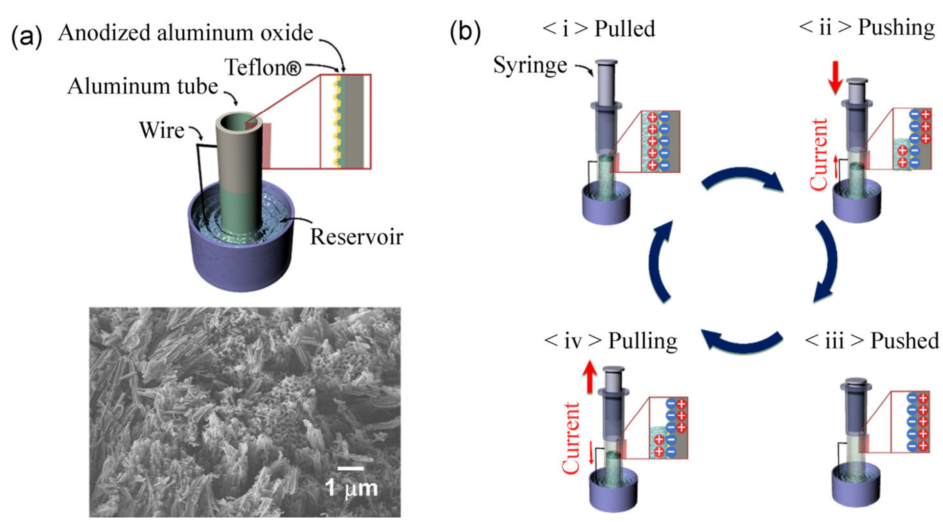

Figure 1 (a) Schematic of the superhydrophobic nanostructured aluminum tube and the scanning electron microscopic (SEM) image of the outermost part of the tube. (b) Working mechanism of the energy harvesting utilizing a superhydrophobic nanostructured aluminum tube. Pulling and pushing of the plunger induce water movement inside the tube.

between the water and the interface. The positive charges inside the aluminum tube located for electrical screening purposes remained. Therefore, the electrons flowed from the reservoir to the aluminum tube to satisfy electroneutrality, as shown in Fig. 1(b) < iv >. Finally, when the surface came into complete contact with water, the developed negative charges were entirely screened by the positive charges inside the water (Fig. 1(b) < i >). An alternating current can be achieved through the reciprocating motion of the syringe plunger and the cyclical movement of electrons. Therefore, electric energy was generated by the coupling of contact electrification and electrostatic induction from the metallic material (i.e., aluminum).

3.2 Energy-harvesting model

The electric current generated by the superhydrophobic nanostructured aluminum tube can be estimated using the charge-current equation:

$$I_{sc} = \frac{dQ}{dt} \tag{1}$$

where I_{sc} is the current generated by dispensing water, Q is the total charge developed by contact electrification between the Teflon and the water, and t is the dispensing time. The developed charge can be calculated as

$$Q = \sigma \times A_{contact} = \sigma \times \pi \times D \times L\left(= \frac{4V}{\pi D^2}\right) = \frac{4\sigma V}{D} \tag{2}$$

where σ is an effective surface charge density of the surface (charge per unit area), $A_{contact}$ is the effective contact area between the superhydrophobic nanostructured surface and the water, D is the aluminum tube diameter, L is the contact length between the Teflon and the water, and V is the total volume of the aspirated water. Given that the wetting behavior of the water inside the aluminum tube is unclear (Cassie state or Wenzel state) because of the heterogeneous nanostructures on the surface, the term "effective surface charge" is used in this study. The effective surface charge density of the surface with various solutions can be easily measured using the Faraday cup method, because the developed charge amount on the surface is the same as that of the dispensed water (see Fig. S1 in the ESM). The total dispensing time of the water can be calculated using the speed of the rotary motor (n rpm). Finally, the estimated short-circuit current, I_{sc}, can be calculated by combining Eqs. (1) and (2):

$$I_{sc} = \frac{Q}{t} = \frac{4\sigma V/D}{30/n} = \frac{2n\sigma V}{15D} \tag{3}$$

With Eq. (3), the generated current can be easily estimated by measuring the charge amount of the dispensed water. The full cyclic movement of the rotary motor generates undesired surface movement of the water such as fluctuations. To avoid this in the experiment, dispensing of the water was only operated by the rotary motor after filling the water by manually pulling the plunger. Under certain experimental conditions (D = 6 mm, V = 2 mL, $\sigma = 1.42 \times 10^{-5}$ C/m^2), the electric current and voltage were measured as plotted in Figs. 2(a) and 2(b). Operating at a dispensing speed of 1,250 rpm, the estimated current calculated by Eq. (3) was approximately 0.79 μA, and the current measured by the experiment was 0.98 μA. The slight difference may be attributed to the following reason. In the model, all water inside the tube was assumed to be instantaneously detached from the tube. However, in reality, water was continuously dispensed from the tube, and the charges inside the aspirated water were also continuously swept during the dispensing stage. During dispensing, the charges may have experienced electrical interactions with the aluminum tube and the separated charges on the contact interface. Because the charge inside the water moved freely compared to the solid, this complicated phenomenon can be considered as an electric coupled dynamic fluid situation. Further study should therefore be performed to fully understand the movement of the charges inside the water during dispensing. Although a slight difference was observed between the experimental data and the theoretical model, the measured current corresponded well with the estimated value.

In Eq. (3), given the effective surface charge density, the major factor that determines electric current is rotary motor speed, which corresponds to the detaching speed of the water because all other parameters are tube properties. Therefore, to investigate the effect of the detaching speed of the water to the electrical output,

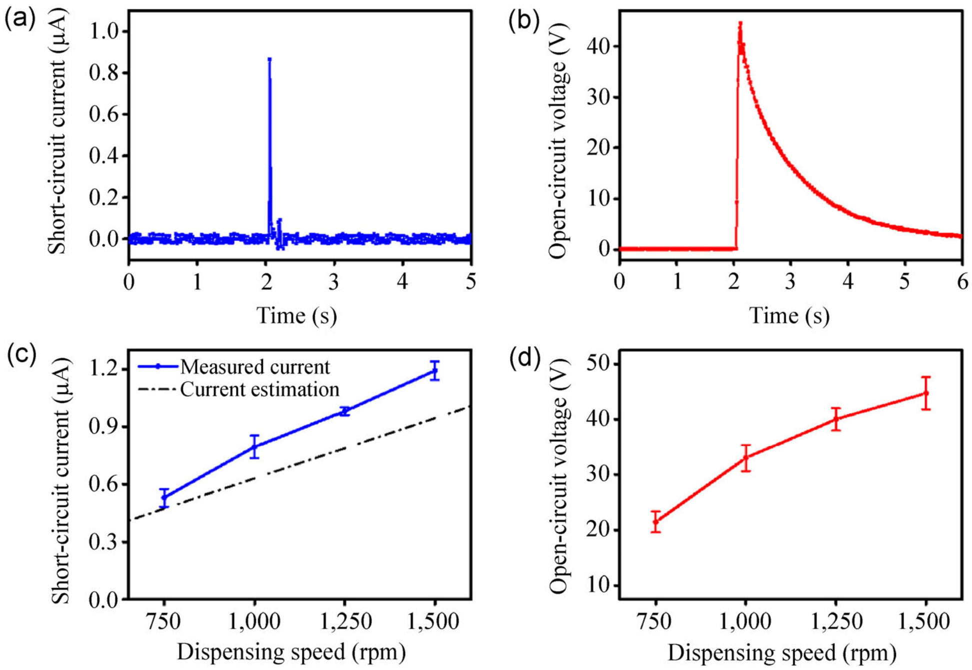

Figure 2 Electrical output generated by the syringe connected to a superhydrophobic nanostructured aluminum tube with 2 mL deionized water. (a) Short-circuit current and (b) open-circuit voltage measurements operating at a dispensing speed of 1,250 rpm. (c) Measurement of short-circuit current while varying dispensing speed. The experimental result shows a linearly proportional relationship. The current comparison shows good agreement between the experimental and theoretical data. (d) Open-circuit voltage measurement. The open-circuit voltage also has a linearly proportional relationship with the dispensing speed of the rotary motor.

the short-circuit current and open-circuit voltage with 2 mL deionized water are measured while varying the rotary motor speed. The experimental result shows a near-linear proportional relationship, as shown in Fig. 2(c). The current comparison indicates good agreement between the experiment and the energy-harvesting model based on Eq. (3). However, the difference between the theoretical model and the experimental result increases with increased detaching speed of the water. This might be attributed to the following reason. In spite of the superhydrophobicity, a small number of positively charged tiny water droplets can remain on the superhydrophobic surface after the detachment of the bulky water from the surface. To support this assumption, an experiment about the remaining tiny water droplets on the superhydrophobic surface and its detachment with shaking motion is additionally performed; the result can be found in the ESM. The remaining water molecules on the superhydrophobic surface can have significant positive charge because of the high electrostatic attraction force between the negatively charged superhydrophobic surface and the positively charged tiny water droplets, thereby affecting to the entire electrical output of the system. The remaining positively charged tiny water droplets played a role of screening the surface charge, resulting in a decrease in effective charge on the surface. These tiny water droplets can be detached with a faster detaching speed. As a result, the effective charge on the surface increased as detaching speed increased. This induced the increase of the short-circuit current; therefore, the difference between the theoretical model and the experimental result increased with increasing detaching speed of the water. Given that this phenomenon might occur in all cases of contact between the superhydrophobic surface and the water, further study of the remaining tiny water droplets on the superhydrophobic surface is needed to fully explain it.

Figure 2(d) shows that the open-circuit voltage is linearly proportional to the dispensing speed of the motor, which corresponds to the detaching speed of the water. This is the first reported finding that both output current and voltage of the SWING have linearly proportional behaviors with the detaching speed of the water. In the previous studies of the TENG utilizing solid–solid contact electrification, measured open-circuit voltage was found to be independent of the contact/separation speed of the solid-phase materials [14, 27]. In terms of solid–water contact electrification, the previous designs led to difficulty in varying the detaching speed of the water to explore the effect of the detaching speed on the electrical output. Even the only report on the effect of contact frequency on output voltage failed to show this relationship because of the generated fluctuating wave on the surface during the operation [19]. The increase of the open-circuit voltage corresponding to the detaching speed of the water can also be explained by the previously mentioned assumption about the remaining tiny water droplets on the superhydrophobic surface. According to the assumption, because the effective charge on the surface increases with increasing detaching speed, there is also an increase in the open-circuit voltage, which is strongly related to the amount of total electric charge on the surface. The increase in the open-circuit voltage also supports the assumption about the remaining tiny water droplets on the superhydrophobic surface.

The results show that the tubular system is useful in exploring the fundamental characteristics of solid–water contact electrification because of the structural advantage gained by varying the detaching speed of the water. The developed energy harvesting model can guide the design parameters for utilizing this system to attain a desired electrical output.

3.3 SWING stick

Utilizing a superhydrophobic nanostructured aluminum tube, the SWING stick, which has the advantage of a compact design, can be easily developed. The compact design of the TENG enables long-lasting operation with a fixed amount of water, which is essential for achieving an evaporation- and contamination-free condition. Recently, the packaging of the TENG became a problem because the operation of the TENG is based on the presence of mechanical triggering, which prevents a compact design. From this viewpoint, the present mechanism based on the movement of water in a tubular system solves this packaging problem.

The water reservoir was attached to the metallic tube (i.e., aluminum) as shown in Fig. 3(a). The connector between the nanostructured tube and the bare aluminum tube was used for sealing; rubber caps bound the two ends of the tubes. The developed SWING stick is a small energy harvester (20 cm^3) with a compact design used to harvest hand-shaking mechanical energy (Fig. 3(b)). Relative motion of the water inside the system from the coated tube to the bare tube, and vice versa, can generate electrical energy

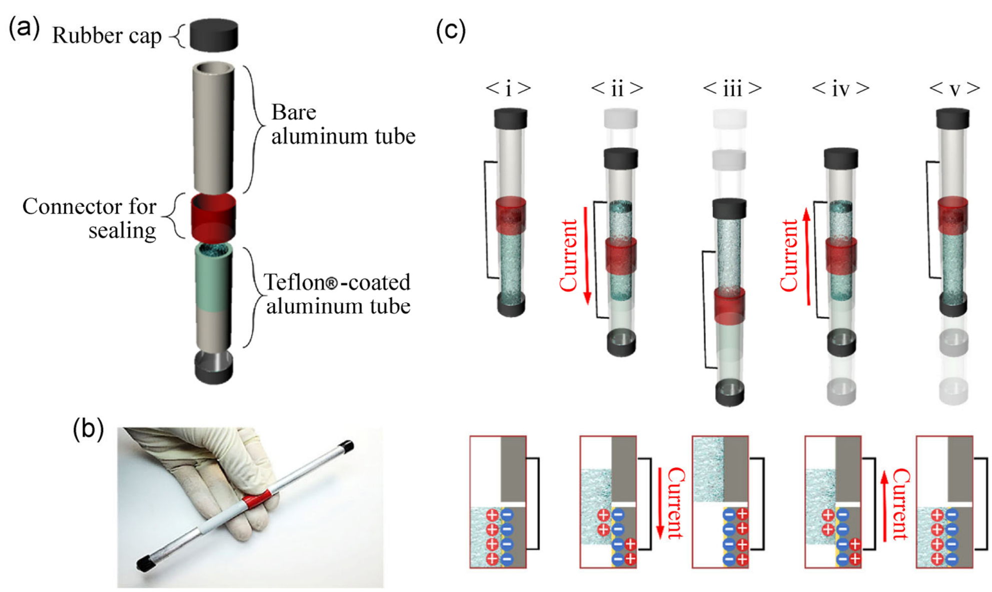

Figure 3 Schematic and working mechanism of the SWING stick. (a) Schematic of the SWING stick. (b) Fabricated SWING stick. (c) Working mechanism of the SWING stick. The relative motion of the water to the SWING stick could generate electric current.

with the following mechanism. Figure 3(c) < i–iii > shows the downward movement of the SWING stick during shaking. In Fig. 3(c) < i >, the water first has full contact with the superhydrophobic aluminum tube. The contact between the Teflon and the water generated the negative charges at the contact surface and positive charges inside the water via contact electrification. As the SWING stick moved downward, the water inside relatively moved upward because of its inertia. The positive charges inside the water could be neutralized with the electrons from the Teflon-coated aluminum tube to satisfy the electroneutrality of the overall SWING stick when water came into contact with the bare aluminum tube, thereby generating the concomitant currents shown in Fig. 3(c) < ii >. Current could no longer be generated after all water was detached from the Teflon-coated aluminum tube and came into contact with the bare aluminum tube. The upward movement of the SWING stick is presented in Fig. 3(c) < iii–v >. As the water moved downward and came into contact with the Teflon-coated aluminum tube again, the electrons moved, and current was generated in the opposite direction.

The developed SWING stick was shaken using hand motion to investigate electrical performance. The electrical output of the SWING stick with a shaking frequency of 13 Hz is represented in Figs. 4(a) and 4(b). The asymmetry of the current is considered because of the different hydrophobicity between the upper (bare aluminum tube) and lower (superhydrophobic aluminum tube) parts of the SWING stick. The superhydrophobicity of the surface directly took part in the detachment of the water, which was a critical factor for generating the current. Operating at a shaking frequency of 13 Hz, the system can produce a peak short-circuit current of 1.3 μA and a peak open-circuit voltage of 18 V. The shaking frequency was measured by analyzing the captured image. According to the theoretical energy harvesting model in Eq. (3), the detachment time of water inside the SWING stick was highly dependent on the movement of the device. Therefore, the relationship between shaking frequency and electrical output is compared in Fig. 4(c). Both electric current and voltage were positively correlated with shaking frequency, as proved above. To demonstrate the concept of the SWING stick, which can be used to harvest energy with various types of water from the environment, the electrical output with tap

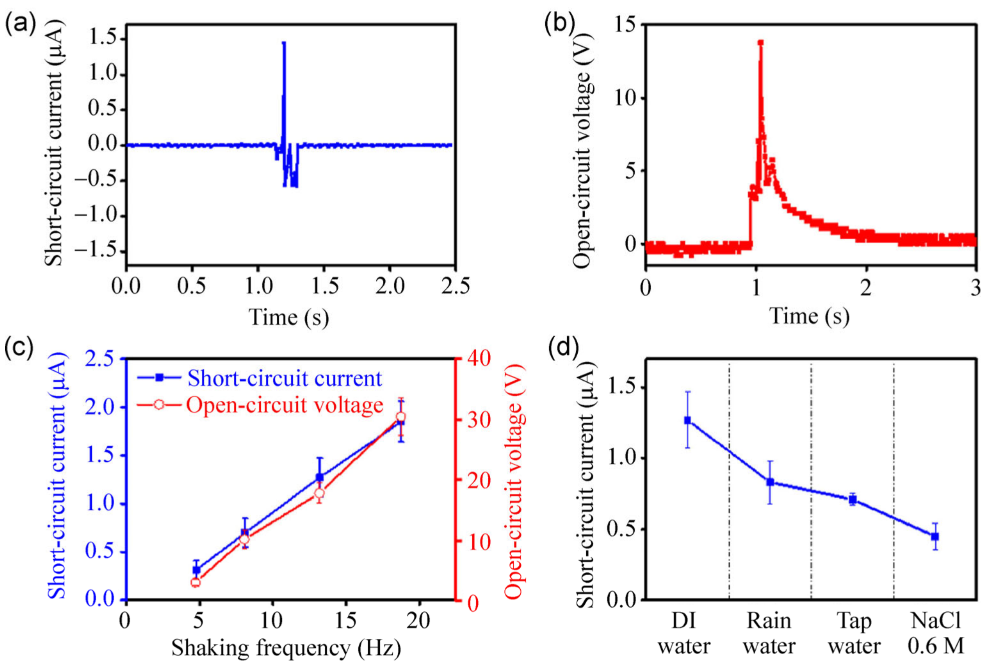

Figure 4 Electrical performance of the SWING stick operated by hand-shaking. (a) Short-circuit current and (b) open-circuit voltage measurements at a shaking frequency of 13 Hz. (c) Measurement of short-circuit current and open-circuit voltage varied at different shaking frequencies. Both short-circuit current and open-circuit voltage have a linearly proportional relationship with shaking frequency. (d) Electrical performance of the SWING stick with various kinds of water from the environment.

water, rainwater, and high concentration (0.6 M, concentration of seawater) of NaCl solution are also compared in Fig. 4(d). The generated electric currents from rainwater, tap water, and electrolyte solution were 65.4%, 55.9%, and 35.4%, respectively, of that of the DI water. These results indicate that electrical output is highly dependent on the electrolyte concentration of the solution. The amount of spontaneously generated charge at the water–solid contact surface was negatively correlated with the electrolyte concentration of the solution based on our previous work [17–18]. Therefore, the amount of electric current related to electrical charge also was negatively correlated with the charges.

The experimental results indicated that the SWING stick can be considered as a viable compact power source. To amplify the electric current, a parallel connection of SWING sticks, called a SWING pack, was demonstrated. Sixteen SWING sticks were electrically connected with conductive epoxy as shown in Fig. 5(a). The electrical outputs of the SWING sticks were measured and are represented in Fig. 5(b)–5(d). The SWING pack can produce a peak short-circuit current of 10 μA and a peak open-circuit voltage of 6 V. Given that the SWING sticks were connected in parallel, the voltages were not amplified, whereas the currents were amplified. Several current peaks appeared in the graph, as shown in Fig. 5(b). These peaks are attributed to the fact that the movement of water inside each SWING stick was not synchronized. Thus, the concomitant current generating times were not the same, with multiple current peaks in one shaking cycle. Hence, the current was not fully amplified because of the differences in peak moments. If the movement of water inside the SWING sticks can be synchronized, then only one peak of the generated current would appear, and the amount of current can be maximized. According to Eqs. (2) and (3), the electrical output is linearly proportional to the inverse of the diameter of the tube. Given that the present technique regarding the fabrication of the superhydrophobic surface can be applied to an aluminum tube with a smaller diameter than that in the present study, a parallel connection of such tubes will significantly increase the electrical output and sensitivity of the system. To power commercially available LEDs, the SWING pack was connected to LEDs as shown in Fig. 5(e). The electrical output generated by shaking the device was sufficient to instantaneously drive the 15 LEDs (see Fig. 5(e), Supporting Video V1). This

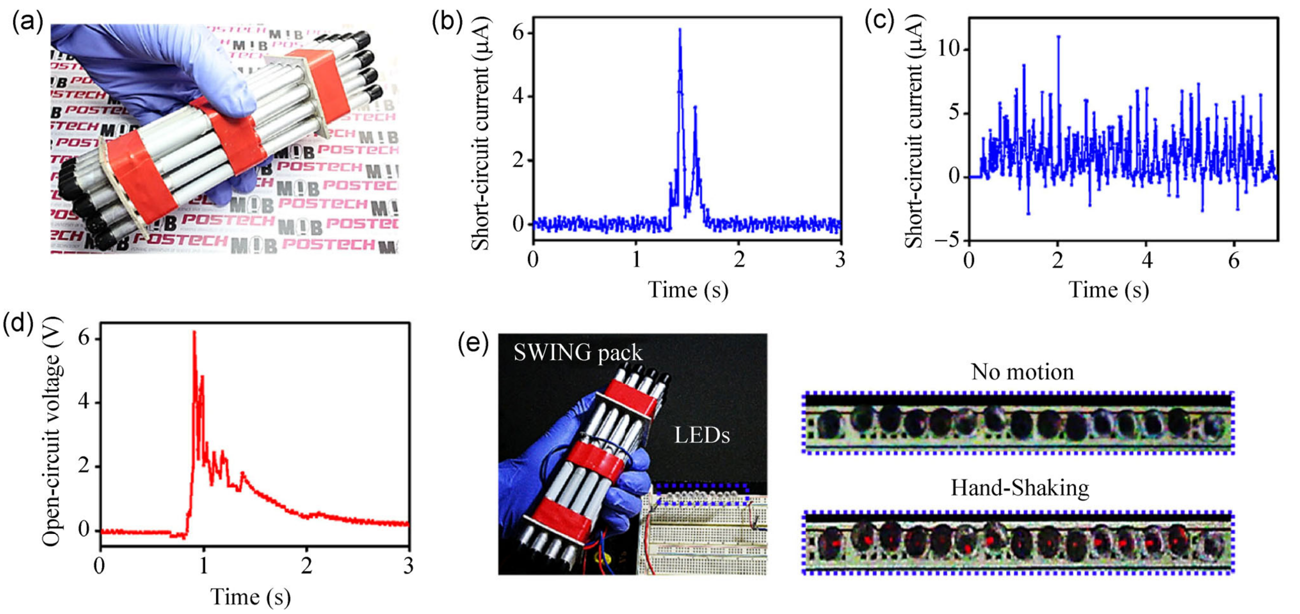

Figure 5 Fabricated SWING pack, 16 SWING sticks connected in parallel, and electrical performance generated from the device operated by hand-shaking. (a) Fabricated SWING pack. The SWING sticks are parallel connected electrically with conductive epoxy. (b) Short-circuit current measurement in one shaking cycle. Multiple current peaks appear in the plot. (c) Short-circuit current and (d) open-circuit voltage measurements. (e) Photograph of the SWING pack as a direct power source to power 15 LEDs.

demonstration suggests a new concept of stick-type nanogenerator using water–solid contact electrification that is small, cost-effective, lightweight, compact, and portable.

4 Conclusions

In this study, the AAO nanostructures on a three-dimensionally curved aluminum surface (tube) were utilized to fabricate a superhydrophobic nanostructured aluminum tube. We then developed a theoretical energy-harvesting model of the moving water inside the tubular system, which is essential for attaining a desired electrical output. The developed model was verified by utilizing the superhydrophobic nanostructured aluminum tube, which has the unique advantage of easy variation of water detaching speed. The linearly proportional relationship between short-circuit current as well as open-circuit voltage and the detaching speed of the water was revealed. Further, this study demonstrated a pioneering stick-type compact TENG to harvest hand-shaking mechanical energy, and the electrical output generated by human hand-shaking motion was measured. Parallel connection of the fabricated SWING sticks, called a SWING pack, enabled easy amplification of electrical output sufficient to power conventional LEDs. A deeper insight into the mechanism and synchronization of water motion among the connected SWING sticks would maximize the electrical output generated by the water-driven fabricated triboelectric nanogenerator. The notable theoretical finding and results shown here would significantly broaden the range of application of triboelectric water-driven nanogenerators.

Acknowledgements

This work was supported by the National Research Foundation of Korea (NRF) grant funded by the Korea government (MSIP). (Nos. 2014R1A2A1A01006527, 2014M3C1B2048632, 2011-0030075) S. Lee: This work was also supported by Basic Science Research Program through the National Research Foundation of Korea (NRF) funded by the Ministry of Education (No. NRF-2014R1A1A2058621). This work was also supported by the Human Resource Training Program for Regional Innovation through the Ministry of Education and National Research Foundation of Korea (NRF-2012H1B8A2026127).

Electronic Supplementary Material: Supplementary material (details of measurement of effective surface charge density, contact angle measurement of the water droplet sitting on the as-treated flat surface, experiment showing tiny water droplets remaining on the superhydrophobic flat surface, and video about lighting up LEDs by using SWING pack as a direct power source) is available in the online version of this article at http: //dx.doi.org/10.1007/s12274-015-0756-4.

References

[1] Brown, K. S. Bright future--or brief flare--for renewable energy? *Science* **1999**, *285*, 678–680.

[2] Dincer, I. Renewable energy and sustainable development: A crucial review. *Renewable Sustainable Energy Rev.* **2000**, *4*, 157–175.

[3] Lund, H. Renewable energy strategies for sustainable development. *Energy* **2007**, *32*, 912–919.

[4] Zhu, G.; Lin, Z.-H.; Jing, Q. S.; Bai, P.; Pan, C. F.; Yang, Y.; Zhou, Y. S.; Wang, Z. L. Toward large-scale energy harvesting by a nanoparticle-enhanced triboelectric nanogenerator. *Nano Lett.* **2013**, *13*, 847–853.

[5] Yang, Y.; Zhu, G.; Zhang, H. L.; Chen, J.; Zhong, X. D.; Lin, Z.-H.; Su, Y. J.; Bai, P.; Wen, X. N.; Wang, Z. L. Triboelectric nanogenerator for harvesting wind energy and as self-powered wind vector sensor system. *ACS Nano* **2013**, *7*, 9461–9468.

[6] Wen, X. N.; Yang, W. Q.; Jing, Q. S.; Wang, Z. L. Harvesting broadband kinetic impact energy from mechanical triggering/vibration and water waves. *ACS Nano* **2014**, *8*, 7405–7412.

[7] Lee, S.; Hong, J. I.; Xu, C.; Lee, M.; Kim, D.; Lin, L.; Hwang, W.; Wang, Z. L. Toward robust nanogenerators using aluminum substrate. *Adv. Mater.* **2012**, *24*, 4398–4402.

[8] Baytekin, H. T.; Patashinski, A. Z.; Branicki, M.; Baytekin, B.; Soh, S.; Grzybowski, B. A. The mosaic of surface charge in contact electrification. *Science* **2011**, *333*, 308–312.

[9] Baytekin, H. T.; Baytekin, B.; Soh, S.; Grzybowski, B. A. Is water necessary for contact electrification? *Angew. Chem. Int. Ed.* **2011**, *50*, 6766–6770.

[10] Terris, B. D.; Stern, J. E.; Rugar, D.; Mamin, H. J. Contact electrification using force microscopy. *Phys. Rev. Lett.*

1989, *63*, 2669.

[11] McCarty, L. S.; Whitesides, G. M. Electrostatic charging due to separation of ions at interfaces: Contact electrification of ionic electrets. *Angew. Chem. Int. Ed.* **2008**, *47*, 2188–2207.

[12] Zhu, G.; Chen, J.; Liu, Y.; Bai, P.; Zhou, Y. S.; Jing, Q. S.; Pan, C. F.; Wang, Z. L. Linear-grating triboelectric generator based on sliding electrification. *Nano Lett.* **2013**, *13*, 2282–2289.

[13] Lin, Z.-H.; Cheng, G.; Wu, W. Z.; Pradel, K. C.; Wang, Z. L. Dual-mode triboelectric nanogenerator for harvesting water energy and as a self-powered ethanol nanosensor. *ACS Nano* **2014**, *8*, 6440–6448.

[14] Zhu, G.; Chen, J.; Zhang, T. J.; Jing, Q. S.; Wang, Z. L. Radial-arrayed rotary electrification for high performance triboelectric generator. *Nat. Commun.* **2014**, *5*, 3426.

[15] Nguyen, V.; Yang, R. S. Effect of humidity and pressure on the triboelectric nanogenerator. *Nano Energy* **2013**, *2*, 604–608.

[16] Bai, P.; Zhu, G.; Liu, Y.; Chen, J.; Jing, Q. S.; Yang, W. Q.; Ma, J. S.; Zhang, G.; Wang, Z. L. Cylindrical rotating triboelectric nanogenerator. *ACS Nano* **2013**, *7*, 6361–6366.

[17] Choi, D.; Lee, H.; Im, D. J.; Kang, I. S.; Lim, G.; Kim, D. S.; Kang, K. H. Spontaneous electrical charging of droplets by conventional pipetting. *Sci. Rep.* **2013**, *3*, 2037.

[18] Choi, D.; Kim, D. S. A zeta (ζ)-pipet tip to reduce the spontaneously induced electrical charge of a dispensed aqueous droplet. *Langmuir* **2014**, *30*, 6644–6648.

[19] Lin, Z. H.; Cheng, G.; Lin, L.; Lee, S.; Wang, Z. L. Water-solid surface contact electrification and its use for harvesting liquid-wave energy. *Angew. Chem. Int. Ed.* **2013**, *52*, 12545–12549.

[20] Cheng, G.; Lin, Z.-H.; Du, Z.-L.; Wang, Z. L. Simultaneously harvesting electrostatic and mechanical energies from flowing water by a hybridized triboelectric nanogenerator. *ACS Nano* **2014**, *8*, 1932–1939.

[21] Zhu, G.; Su, Y. J.; Bai, P.; Chen, J.; Jing, Q. S.; Yang, W. Q.; Wang, Z. L. Harvesting water wave energy by asymmetric screening of electrostatic charges on a nanostructured hydrophobic thin-film surface. *ACS Nano* **2014**, *8*, 6031–6036.

[22] Kwon, S. H.; Park, J.; Kim, W. K.; Yang, Y. J.; Lee, E.; Han, C. J.; Park, S. Y.; Lee, J.; Kim, Y. S. An effective energy harvesting method from natural water motion active transducer. *Energy Environ. Sci.* **2014**, *7*, 3279–3283.

[23] Lin, Z. H.; Cheng, G.; Lee, S.; Pradel, K. C.; Wang, Z. L. Harvesting water drop energy by a sequential contact-electrification and electrostatic-induction process. *Adv. Mater.* **2014**, *27*, 4690–4696.

[24] Kim, Y.; Lee, S.; Cho, H.; Park, B.; Kim, D.; Hwang, W. Robust superhydrophilic/hydrophobic surface based on self-aggregated Al_2O_3 nanowires by single-step anodization and self-assembly method. *ACS Appl. Mater. Interfaces* **2012**, *4*, 5074–5078.

[25] Ravelo, B.; Duval, F.; Kane, S.; Nsom, B. Demonstration of the triboelectricity effect by the flow of liquid water in the insulating pipe. *J. Electrost.* **2011**, *69*, 473–478.

[26] Yatsuzuka, K.; Mizuno, Y.; Asano, K. Electrification phenomena of pure water droplets dripping and sliding on a polymer surface. *J. Electrost.* **1994**, *32*, 157–171.

[27] Zhu, G.; Zhou, Y. S.; Bai, P.; Meng, X. S.; Jing, Q. S.; Chen, J.; Wang, Z. L. A shape-adaptive thin-film-based approach for 50% high-efficiency energy generation through micro-grating sliding electrification. *Adv. Mater.* **2014**, *26*, 3788–3796.